Error Quantification and Control for Adaptive Kriging-Based Reliability Updating with Equality Information

Chi Zhang¹, Zeyu Wang², Abdollah Shafieezadeh¹

¹ Risk Assessment and Management of Structural and Infrastructure Systems (RAMSIS) Lab, Department of Civil, Environmental, and Geodetic Engineering, The Ohio State University, Columbus, OH, 43210, United States
² Department of Civil Engineering, Tsinghua University, Beijing, 100084, China

ABSTRACT

New information obtained through measurements provide an opportunity to update estimates of a system's reliability. For equality type information, reliability updating is a daunting task. The current state-of-art method, reliability updating with equality information using adaptive Kriging (RUAK), integrates an adaptive Kriging process with a transformation of equality information into inequality information. The stopping criterion for training the Kriging model relies on the estimated error for prior failure probability, thus leaving the potential for the true error in posterior failure probability to exceed acceptable thresholds. This study presents a method to estimate, for a given confidence level, the maximum error in posterior failure probability in adaptive Kriging-based reliability updating. Moreover, a two-phase approach is proposed for active learning and adaptive training of Kriging models in reliability updating problems. The new stopping criterion based on the maximum error of posterior failure probability ensures the accuracy of Kriging and thus the reliability estimates, while the two-phase scheme avoids unnecessary training hence improving the efficiency of reliability updating. Four numerical examples are considered to investigate the performance of the proposed approach. It is demonstrated that this method offers the ability to balance between the accuracy of reliability estimates and the computational demand.

Key words: Reliability updating; Reliability analysis, Surrogate model; Adaptive Kriging, Posterior probability error; Measurements; Monitoring

1. Introduction

Real-world systems are typically under the influence of uncertainties. In the reliability domain, the probability of failure quantifies the probability of a system failing to meet a specific performance requirement. It is a vital measurement of performance that considers uncertainties. Let $\mathbf{X} = [X_1, X_2, ..., X_n]$ denote the continuous random variable vector representing the uncertainties with joint probability density function $f_{\mathbf{X}}(\mathbf{x})$. The failure probability of interest, denoted as Pr(E) or P_f , can be defined as:

$$P_f = Pr(E) = Pr(g(X) \le 0) = \int_{x \in \Omega_E} f_X(x) dx \tag{1}$$

where E is the failure event whose domain is denoted as Ω_E , and g(X) is the limit state function representing the status of the system. Reliability analysis methods can be categorized into three groups: approximation methods, simulation methods and metamodel-based methods [1]. Approximation methods, such as first and second order reliability method (FORM and SORM)) [2], [3] approximate the limit state function using Taylor series expansion. These techniques are efficient, but they can be inaccurate for highly nonlinear problems due to the approximation error. Simulation methods such as Monte Carlo Simulation (MCS) [4], Importance Sampling (IS) [4] and Subset Simulation are often used; however, they are computationally costly as they require numerous model evaluations to ensure small coefficient of variation; IS also requires an accurate importance distribution, which may be difficult to acquire. Metamodel-based methods use limited model evaluations to construct metamodels, also referred to as surrogate models, to mimic the behavior of the original time-consuming limit state functions and subsequently to estimate the failure probability. This group of methods can be both efficient and accurate for problems that do not involve large scale or discontinuous responses if a surrogate model is well-constructed in an efficient manner. Polynomial Response Surface [5]-[7], Polynomial Chaos Expansion (PCE) [8], Support Vector Regression (SVR) [9], [10], and Kriging [11] are among popular surrogate models. Kriging surrogate model, because of its ability to provide uncertainty information, has gained significant popularity in the community of reliability analysis in the recent decade. Inspired by Jones et al. [12], Bichon et al. [13] proposed Efficient Global Reliability Analysis that used Kriging model to perform reliability analysis. Echard et al. [11] developed an active learning reliability method combining Kriging and Monte Carlo Simulation (AK-MCS) where the famous U' learning function was proposed. Bect et al. [14] derived stepwise uncertainty reduction strategies from a Bayesian formulation of the reliability analysis problem. Picheny et al. [15] proposed an adaptive strategy to build a Kriging model based on an explicit trade-off between reduction in global uncertainty and exploration of regions of interest. Gaspar et al. [16] showed that Kriging models provide gains of accuracy and efficiency for structural reliability analysis. Gaspar et al. [17] proposed an adaptive Kriging-based trust region method to search for the design point with IS. Xiao et al. [18] used active learning Kriging to address system reliability based-design optimization problems.

For existing structures, circumstances can arise when it becomes necessary to re-evaluate the reliability. Such circumstances can include, among others, when damages are observed, the use of the structure is to be changed, or the life time is extended [2]. Information about the state of systems and their properties or their environment collected through observations and monitoring has become more available. This information can be used to re-evaluate the reliability of systems. In reliability updating, the posterior failure probability represents the probability of a structure or system failing given such information. The posterior failure probability can be calculated using the following equation:

$$P_{f}' = \frac{Pr(E \cap Z)}{Pr(Z)} = \frac{\int_{x \in \{\Omega_{E} \cap \Omega_{Z_{1}} \cap \dots \cap \Omega_{Z_{m}}\}} f_{X}(x) dx}{\int_{x \in \{\Omega_{Z_{1}} \cap \dots \cap \Omega_{Z_{m}}\}} f_{X}(x) dx}$$
where Z represents the observation of intersection of events $Z_{1}, Z_{2}, \dots, Z_{m}$ whose domains are defined as

where Z represents the observation of intersection of events $Z_1, Z_2, ..., Z_m$ whose domains are defined as $\Omega_{Z_1}, \Omega_{Z_2}, ..., \Omega_{Z_m}$, respectively. The information here is often of two types: inequality information and equality information [19]. The information Z_i can be categorized as inequality, if it can be formulated as follows:

$$\Omega_{Z_i} = \{ h_i(\mathbf{x}) \le 0 \} \tag{3}$$

where $h_i(x)$ denotes the information function. An example of inequality information is that no defect is observed, i.e., the system response minus the critical value is smaller than zero. On the other hand, equality information is often representative of quantitative measurements of system characteristics, and can be formulated as follows:

$$\Omega_{Z_i} = \{ h_i(\mathbf{x}) = 0 \} \tag{4}$$

Between the two types, the inequality one is easier to deal with, and the posterior probability of failure given inequality information can be estimated using conventional reliability methods. The main difficulty of reliability updating lies in how to handle equality information: if one of the Z_i s is of the equality type, the integrals in both denominator and numerator in Eq. (2) will become zero. In other words, the domain Ω_Z is a surface in the space of \boldsymbol{x} if any of the information event is of the equality type. Thus, Eq. (2) cannot be solved directly using traditional structural reliability methods mentioned above. It should be noted that there are two viewpoints toward the estimation of P_f . The first approach is to directly perform reliability updating using Eq. (2). The other approach involves updating the distribution of the random variables with Bayesian updating and then performing reliability analysis with the updated distribution. The latter method is obviously computationally very demanding compared to the first approach [20].

A number of techniques have been proposed to solve reliability updating with equality information. Madsen [21] showed that the posterior probability of failure can be estimated using the partial derivatives of the probabilities by introducing a dummy parameter. However, this approach can lead to significant errors and is not practical in many cases [19]. In Strurel software [22], first-order and second order approximations to surface integration are used, and this approach offers acceptable efficiency and accuracy for linear reliability problems. However, for nonlinear problems, the error of this approach may not be negligible. Straub [19] proposed a new approach by transferring the equality information into inequality information with an auxiliary standard normal random variable. This method facilitates updating reliability by converting the original problem into two traditional structural reliability problems. It achieves sufficient accuracy and efficiency with simulation methods [19]. However, there are two main drawbacks for the method. First, the numerator of Eq. (2) is concerned with the probability of a joint event, which is typically a rare event with a very small probability. Thus, a large number of function evaluations are needed in the simulation methods. Moreover, re-evaluation of the numerator in Eq. (2) is required when new information becomes available, increasing the number of limit state function evaluations. To overcome the aforementioned limitations, Wang and Shafieezadeh [20] proposed an efficient metamodel-based reliability updating approach called Reliability Updating with equality information using Adaptive Kriging (RUAK). RUAK uses Straub's information type transformation [19] and integrates an adaptive Kriging approach into reliability updating. The adaptive Kriging approach refines the surrogate model adaptively by adding a training point in each iteration until a certain stopping criterion is satisfied. RUAK uses an error-based stopping criterion (ESC) [23], which involves the maximum error of the prior failure probability. As the posterior failure probability is the final outcome of reliability updating, using ESC has the potential to lead to an immature stop of the surrogate model construction, and hence an inaccurate posterior failure probability

In applications concerning reliability analysis and updating, reaching 'acceptable' accuracy often supersedes computational efficiency as an unacceptably inaccurate result will have no or very limited value no matter how efficiently it is derived. Without an approach to estimate the error, it will be unknown to what degree the results are reliable and useful. While methods such as Reliability analysis through Error rate-based Adaptive Kriging (REAK)

[24] and ESC have been developed for error quantification in reliability analysis methods, no such method currently exists for reliability updating. Therefore, an approach is needed to reliably estimate error in posterior failure probability and integrate this estimate in the stoppage criteria of adaptive analyses. This capability will allow the user to strike a balance between the desired accuracy and computational demand.

This paper proposes a method to estimate the maximum error of posterior failure probability for Kriging-assisted reliability updating with equality information. The maximum error here is derived for a given confidence level and is incorporated as the stopping criterion for the adaptive construction of the surrogate model used in reliability updating. The approach also leverages a two-phase scheme to avoid unnecessary calls to the limit state function. The performance of the proposed method is demonstrated through four numerical examples in comparison with the original RUAK. The rest of the paper is organized as follows. Section 2 provides a review of the Kriging surrogate model, ESC and RUAK. Section 3 introduces the proposed method for estimating the maximum error of posterior failure probability. The following section presents the two-phase approach to reliability updating. Four numerical examples are discussed in Section 5. Section 6 provides the conclusions of this study.

2. Reliability Updating using Adaptive Kriging

This section first introduces the Kriging surrogate model. Then, ESC and RUAK approach are reviewed.

2.1 The Kriging surrogate model

Kriging surrogate models have gained popularity in metamodel-based reliability analysis-related studies [11], [20], [24]–[27]. In those methods, the limit state function g(X), which is usually evaluated using a time-consuming finite element model, can be regarded as a draw of a Gaussian process. A Kriging surrogate model $\hat{g}(X)$ can be described by the following equation [28]:

$$\hat{g}(X) = \beta^T f(X) + Z(X) \tag{5}$$

where f(X) is the Kriging basis that consists of p arbitrary functions $f_i(X)$, i = 1, 2, ..., p, β is the vector of corresponding set of coefficients β_i , i = 1, 2, ..., p, $\beta^T f(X)$ represents the long term trend and Z(x) is a stationary Gaussian process. The trend can have formulations including constant (β_0) , linear $(\beta_0 + \sum_{i=1}^n \beta_i x_i)$ and quadratic $(\beta_0 + \sum_{i=1}^n \beta_i x_i + \sum_{i=1}^n \sum_{j=1}^i \beta_{ij} x_i x_j)$ [29]. The Gaussian process Z(X) has a zero mean and a covariance matrix that can be represented as:

$$COV\left(Z(\mathbf{x}^{(i)}), Z(\mathbf{x}^{(j)})\right) = \sigma^2 R(\mathbf{x}^{(i)}, \mathbf{x}^{(j)}; \boldsymbol{\theta})$$
(6)

where σ^2 is the process variance and $R(\mathbf{x}^{(i)}, \mathbf{x}^{(j)}; \boldsymbol{\theta})$ is the correlation function of two points $\mathbf{x}^{(i)}, i = 1, 2, ..., N_{mcs}$ and $\mathbf{x}^{(j)}, j = 1, 2, ..., N_{mcs}$ in the candidate design points \boldsymbol{S} generated through MCS with hyper parameters $\boldsymbol{\theta}$. The correlation function used in this paper is the Gaussian correlation function, which can be formulated as follows:

$$R(\mathbf{x}^{(i)}, \mathbf{x}^{(j)}; \boldsymbol{\theta}) = \prod_{k=1}^{n} \exp\left(-\theta^{k} \left(x_{k}^{(i)} - x_{k}^{(j)}\right)^{2}\right)$$
 (7)

where $x_k^{(i)}$ is the k_{th} dimension of $\mathbf{x}^{(i)}$, and θ^k is the k_{th} hyperparameter. When θ^k are the same, R is called an isotropic correlation function, otherwise, it is called an anisotropic correlation model. In this paper, the anisotropic correlation function is used in which θ^k , k = 1, 2, ..., n can be different.

With a set of m training points $[\mathbf{x}_{tr}^{(1)}, \mathbf{x}_{tr}^{(2)}, ..., \mathbf{x}_{tr}^{(m)}]$ and the corresponding function values $\mathbf{Y} = [g(\mathbf{x}_{tr}^{(1)}), g(\mathbf{x}_{tr}^{(2)}), ..., g(\mathbf{x}_{tr}^{(m)})]$, $\boldsymbol{\beta}$ and σ^2 can be calculated using the following equations [12]:

$$\boldsymbol{\beta} = (\boldsymbol{F}^T \boldsymbol{R}^{-1} \boldsymbol{F})^{-1} \boldsymbol{F}^T \boldsymbol{R}^{-1} \boldsymbol{Y} \tag{8}$$

$$\sigma^2 = \frac{1}{m} (\mathbf{Y} - \mathbf{F} \boldsymbol{\beta})^T \mathbf{R}^{-1} (\mathbf{Y} - \mathbf{F} \boldsymbol{\beta})$$
(9)

where F is the matrix of f(X) with $F_{ij} = f_j(x_{tr}^{(i)})$, i = 1, 2, ..., m, j = 1, 2, ..., p, and R is the autocorrelation matrix with $R_{ij} = R(x_{tr}^{(i)}, x_{tr}^{(j)}; \theta)$, i = 1, 2, ..., m, j = 1, 2, ..., m. As β and σ^2 depend on θ through R, it is required to obtain the values in θ . In this paper, θ is estimated through maximum likelihood estimation (MLE) method [30]. The formulation based on MLE is as follows:

$$\boldsymbol{\theta}^* = \underset{\boldsymbol{\theta}}{\operatorname{argmin}} \left(\left| \boldsymbol{R} (\boldsymbol{x}_{tr}^{(i)}, \boldsymbol{x}_{tr}^{(j)}; \boldsymbol{\theta}) \right|^{\frac{1}{m}} \sigma^2 \right)$$
 (10)

The optimization method used to solve the problem is genetic algorithm [31]. Given the results of the optimization problem, for an unknown point x, the predicted function value through the Kriging model can be estimated using the following equation [29]:

$$\mu_{\hat{g}}(\mathbf{x}) = \mathbf{f}^{T}(\mathbf{x})\mathbf{\beta} + \mathbf{r}^{T}(\mathbf{x})\mathbf{R}^{-1}(\mathbf{Y} - \mathbf{F}\mathbf{\beta})$$
(11)

where r(x) is the correlation vector between x known training points $x_{tr}^{(i)}$, i = 1, 2, ..., m with $r_i(x) = R(x, x_{tr}^{(i)}; \theta)$. Note that $\mu_{\hat{g}}$ is the mean value of the predicted function value with variance of $\sigma_{\hat{g}}^2$ [29]:

$$\sigma_{\hat{\sigma}}^{2}(x) = \sigma^{2}(1 + u^{T}(x)(F^{T}R^{-1}F)^{-1}u(x) - r^{T}(x)R^{-1}r(x))$$
(12)

where $u(x) = F^T R^{-1} r(x) - f(x)$. The predicted function values all follow a normal distribution with the mean and variances estimated using Eq. (11) and Eq. (12). Once a well-constructed Kriging surrogate model is obtained, simulation methods such as MCS can be used to estimate the failure probability with the surrogate model replacing the original time-consuming model.

During the process of the model construction, uncertainty information offered by the Kriging model can help with the identification of the next best training points and the stopping criterion for the construction of the surrogate model for reliability analysis. Echard et al. [11] proposed the U' learning function with the following form:

$$U'(x) = \frac{|\mu_{\hat{g}}(x)|}{\sigma_{\hat{g}}(x)} \tag{13}$$

The U' learning function identifies points that are close to the limit state, have high uncertainty or both at the same time. The U' learning function represents a reliability index for the risk of making wrong sign estimation of the limit state function. The point with the smallest U' learning function, i.e., the point whose sign of the limit state function value has the highest probability of being wrongly estimated, is regarded as the next best training point. The U' learning function can also be used as Kriging model's stopping criterion, which is defined as $min(U'(x)) \ge 2$. When the stopping criterion is satisfied, the Kriging model is deemed to be sufficiently accurate. When the stopping criterion is not satisfied, a new training point is added for the construction of the surrogate model. This approach, which gradually adds training points to refine the surrogate model until some stopping criterion is satisfied, is regarded as adaptive Kriging. However, most existing stopping criteria do not directly relate to the error in estimated failure probabilities. Wang and Shafieezadeh [23] proposed an error-based stopping criterion (ESC) to address this limitation. The stopping criterion is reviewed in the next subsection.

2.2 The Error-based stopping criterion

Wang and Shafieezadeh [23] proposed the ESC that estimates the maximum error of failure probability introduced by the Kriging model. ESC stops the surrogate model construction when the estimated maximum error of failure probability is smaller than a predefined threshold ϵ_{thr} . In ESC, the maximum error for the failure probability estimated using the Kriging surrogate model is determined using the following equation:

$$\hat{\epsilon}_{max} = max \left(\left| \frac{\hat{N}_f}{\hat{N}_f - \hat{S}_f^u} - 1 \right|, \left| \frac{\hat{N}_f}{\hat{N}_f + \hat{S}_S^u} - 1 \right| \right)$$
(14)

where \widehat{N}_f is the estimated number of failure points by the surrogate model in the MCS population, \widehat{S}_f^u and \widehat{S}_s^u are the upper bounds of \widehat{S}_f and \widehat{S}_s , respectively, and \widehat{S}_f and \widehat{S}_s are the total number of wrong sign estimations in the estimated failure and safe domains $\widehat{\Omega}_f$ and $\widehat{\Omega}_s$, respectively. Wang and Shafieezadeh [23] showed that \widehat{S}_s and \widehat{S}_f follow two Poisson binomial distributions with mean and variance shown below, respectively:

$$\hat{S}_s \sim PB\left(\sum_{i=1}^{\hat{N}_s} P_i^{wse}, \sum_{i=1}^{\hat{N}_s} P_i^{wse} \left(1 - P_i^{wse}\right)\right)$$

$$\tag{15}$$

$$\hat{S}_{f} \sim PB \left(\sum_{i=1}^{\hat{N}_{f}} P_{i}^{wse}, \sum_{i=1}^{\hat{N}_{f}} P_{i}^{wse} \left(1 - P_{i}^{wse} \right) \right)$$
(16)

where PB denotes the Poisson Binomial distribution, \widehat{N}_s is the number of points in $\widehat{\Omega}_s$, and P_i^{wse} denotes the probability of wrong sign estimation for $\mathbf{x}^{(i)}$ in \mathbf{S} , which can be calculated as:

$$P_i^{wse} = \Phi\left(-U'(\mathbf{x}^{(i)})\right) \tag{17}$$

where $\Phi(\cdot)$ is the cumulative density function (CDF) of a standard normal distribution. Therefore, given a significance level α (usually 5%), the upper and lower bounds of \hat{S}_s and \hat{S}_f can be found as:

$$\hat{S}_s \in [\boldsymbol{\theta}_{\hat{S}_s}^{-1} \left(\frac{\alpha}{2}\right), \boldsymbol{\theta}_{\hat{S}_s}^{-1} \left(1 - \frac{\alpha}{2}\right)] \tag{18}$$

$$\hat{S}_f \in [\boldsymbol{\theta}_{\hat{S}_f}^{-1} \left(\frac{\alpha}{2}\right), \boldsymbol{\theta}_{\hat{S}_f}^{-1} \left(1 - \frac{\alpha}{2}\right)] \tag{19}$$

where $\boldsymbol{\theta}_{\hat{S}_s}^{-1}$ and $\boldsymbol{\theta}_{\hat{S}_f}^{-1}$ are the inverse CDFs of the two Poisson Binomial distributions. For more details for the computation of $\hat{\epsilon}_{max}$, readers are referred to [23].

The RUAK approach, which uses ESC as the stopping criterion, is introduced in the next subsection.

2.3 Reliability updating using adaptive Kriging

Wang and Shafieezadeh [20] proposed RUAK to estimate the posterior failure probability. In RUAK, using the Bayes' theorem the posterior failure probability P'_f breaks down into three components: prior failure probability P_f , probability of observations Pr(Z), and conditional probability of observations Pr(Z|E). The estimated posterior failure probability \hat{P}'_f by the Kriging model can be represented as:

$$\hat{P}_f' = \frac{\widehat{Pr}(Z|E) \cdot \widehat{P}_f}{Pr(Z)} \tag{20}$$

where $\widehat{Pr}(Z|E)$ is the estimated Pr(Z|E) where the failure event E is determined by the Kriging model, and \widehat{P}_f is the corresponding estimated prior failure probability. Note that "^" herein denotes that the value under is determined by the Kriging model and carries the error as a result of the Kriging model. Therefore, based on the well-constructed surrogate model $\hat{g}(X)$, \hat{P}_f can be estimated as:

$$\hat{P}_f = \frac{\sum_{i=1}^{N_{mcs}} I_{\hat{g}}(\boldsymbol{x}^{(i)})}{N_{mcs}} \tag{21}$$

where $I_{\hat{g}}(\cdot)$ is the corresponding indicator function:

adicator function:

$$l_{\hat{g}}(\boldsymbol{x}^{(i)}) = \begin{cases} 1, & \text{when } \hat{g}(\boldsymbol{x}^{(i)}) \leq 0\\ 0, & \text{when } \hat{g}(\boldsymbol{x}^{(i)}) > 0 \end{cases}$$
(22)

For the calculation of Pr(Z), RUAK adopts equality information transformation in [19]. Pr(Z) can be explicitly obtained via MCS:

$$Pr(Z) = \frac{q}{c_1} \cdot \frac{\sum_{i=1}^{N_{mcs}} I_Z(\mathbf{x}^{(i)}, p_i)}{N_{mcs}}$$
 (23)

where q is a constant representing proportional relationship between Pr(Z|X=x) and the likelihood function L(x)of the observation Z. Note that Z here is independent of the failure event, thus the Kriging model is not involved here. L(x) corresponds to the information function h(x) = 0 and can be expressed as $L(x) = f_{\varepsilon}(s_m - s(x))$, with f_{ε} being the probability density function of the measurement error ε , s_m being the measurement of a property in Z and s(x)being the property expressed in terms of \mathbf{x} , which can be \mathbf{x} or any function of \mathbf{x} . Moreover, $c_1 = \frac{1}{\max(L(\mathbf{x}))}$ and $I_Z(\cdot)$ is the corresponding indicator function expressed as:

where
$$h_e(\cdot)$$
 is an augmented limit state function for transforming equality information into inequality information:
$$I_z(x_i, p_i) = \begin{cases} 1, & \text{when } h_e(x^{(i)}, p_i) \leq 0 \\ 0, & \text{when } h_e(x^{(i)}, p_i) > 0 \end{cases}$$
 where $h_e(\cdot)$ is an augmented limit state function for transforming equality information into inequality information:

$$h_e(\mathbf{x}, p) = p - c_1 L(\mathbf{x}) \tag{25}$$

where p is an auxiliary standard uniform random variable. Thus, Pr(Z) herein is regarded as the probability of failure according to the augmented limit state function $h_e(\cdot)$. Similarly, the probability of the observations conditional on the failure event $\hat{P}r(Z|E)$ can be determined using MCS as follows:

$$\widehat{P}r(Z|E) = \frac{q}{c_2} \cdot \frac{\sum_{j=1}^{\widehat{N}_f} I_{\widehat{Z}^+}(\mathbf{x}^{\prime(j)}, p_j)}{\widehat{N}_f}$$
 (26)

where x' are the points in $\widehat{\Omega}_f$, which is determined by the Kriging model $\widehat{g}(X)$, $c_2 = \frac{1}{\max(L(x'))}$ and $I_{Z+}(\cdot)$ is the indicator function given by:

$$I_{\hat{Z}^{+}}(\mathbf{x}^{\prime(j)}, p_{j}) = \begin{cases} 1, & \text{when } \hat{h}_{e}^{+}(\mathbf{x}^{\prime(j)}, p_{j}) \leq 0\\ 0, & \text{when } \hat{h}_{e}^{+}(\mathbf{x}^{\prime(j)}, p_{j}) > 0 \end{cases}$$
 (27)

where $\hat{h}_e^+(\cdot)$ is the second augmented limit state function corresponding to the transformation from equality information into inequality one:

$$\hat{h}_{e}^{+}(p, \mathbf{x}') = p - c_{2}L(\mathbf{x}') \tag{28}$$

Note that $\hat{h}_e^+(\cdot)$ carries the error introduced by the Kriging model as all points considered herein are the failure points x' according to the Kriging model $\hat{g}(X)$ of the actual limit state function g(X). Thus, $\hat{P}r(Z|E)$ herein is regarded as the probability of failure according to the second augmented limit state function $\hat{h}_e^+(\cdot)$ for points in $\hat{\Omega}_f$. Once all three components are obtained, \hat{P}'_f can be easily calculated using Eq. (20). The reader is referred to Wang and Shafieezadeh [20] for more detail.

This methodology has two main advantages: (1) estimations of P_f and Pr(Z|E) are computationally efficient and (2) once the estimation of \hat{P}_f is ready, reliability updating becomes efficient whenever the observations and information are changing. However, this method has one main drawback: it uses ESC as the stopping criterion for the construction of Kriging surrogate model, and ESC only considers the error of the prior probability of failure \hat{P}_f whereas the posterior failure probability \hat{P}_f' is of interest. In the three components required to calculate \hat{P}_f' , $\hat{Pr}(Z|E)$ is estimated using points in the estimated failure domain, which is determined by the Kriging model. The wrong sign estimation will affect not only \hat{P}_f , but also $\hat{Pr}(Z|E)$. The actual error of \hat{P}_f' can be larger than the maximum error of \hat{P}_f estimated by ESC. This drawback may lead to an immature stoppage of training of the surrogate model. Thus, an estimation of the maximum error of \hat{P}_f' is desired to be used as the stopping criterion for the Kriging model construction for reliability updating. In this paper, we propose a method to estimate the maximum error of the final output \hat{P}_f' . The method is introduced in the next section.

3. Error Estimation for the Posterior Failure Probability

As mentioned in Section 2, using the surrogate model may introduce errors due to the potential for wrong estimation of the domain of sample points. The maximum error of the posterior failure probability cannot be easily estimated. Here, it is proposed to evaluate the error of conditional probability $\widehat{Pr}(Z|E)$ first. Once the maximum error of $\widehat{Pr}(Z|E)$ is obtained, given the maximum error of prior failure probability offered by ESC, the maximum error of $\widehat{Pf}(Z|E)$ can be easily estimated. Before introducing the approach for estimating the error of $\widehat{Pr}(Z|E)$, the source of error is discussed first.

In estimating Pr(Z|E), the error occurs when the sample points in the MCS population are misclassified in the prior failure probability estimation. First, $\widehat{Pr}(Z|E)$ is calculated using the points that are determined by the surrogate model to be in the failure domain, thus misclassified points in both $\widehat{\Omega}_f$ and $\widehat{\Omega}_s$ can have an impact on the accuracy of the conditional probability estimation. The actual points in failure domain can be obtained by adding points that are misclassified in the survival domain to the failure domain and removing points that are misclassified in the failure domain. Second, according to Eq. (26), c_2 depends on the value of max(L(x')), which may also be affected when adding and removing misclassified points with large likelihood function values. The error of $\widehat{Pr}(Z|E)$ can therefore be calculated as follows:

$$\hat{\epsilon}_{max}^{\Pr(Z|E)} = \left| \frac{\hat{P}r(Z|E) - Pr(Z|E)^*}{Pr(Z|E)^*} \right| = \left| \frac{\frac{1}{\hat{c}_2} \frac{\hat{N}_{f+}}{\hat{N}_f} - \frac{1}{c_2^*} \frac{N_{f+}}{N_f}}{\frac{1}{c_2^*} \frac{N_{f+}}{N_f}} \right|$$
(29)

where $Pr(Z|E)^*$ is the true value of Pr(Z|E), \widehat{N}_{f+} is the number of estimated failure points that 'fail' again according to the limit state Eq. (28), i.e., $\widehat{h}_e^+(p_j, \mathbf{x}'^{(j)}) \leq 0$, (hereafter abbreviated as LSFI), N_{f+} is the true counterpart, \widehat{c}_2 is the estimated value of the constant in Eq. (26), and c_2^* is the true counterpart.

estimated value of the constant in Eq. (26), and c_2^* is the true counterpart.

According to Eq. (29), the estimation of $\hat{\epsilon}_{max}^{Pr}(^{Z|E)}$ is achievable once the estimate of the range of Pr $(Z|E)^*$ is known. Given that q is the proportionality constant that will be canceled out, the problem can be transferred into estimating the range of $Pr(Z|E)^*/q$, i.e., $\frac{1}{c_2^*} \frac{N_{f^+}}{N_f}$, which can be seen as the product of $\frac{1}{c_2^*}$ and $\frac{N_{f^+}}{N_f}$. The first term is quite straightforward and can be regarded as a monotone decreasing function for $c_2^* > 0$. The main difficulty lies in the estimation of the range of the second term $\frac{N_{f^+}}{N_f}$. The derivation of the bounds is presented next.

3.1 Upper bound of N_{f+}/N_f

First consider Case 1, in which \hat{S}_f^u points in $\hat{\Omega}_f$ are misclassified. Thus, \hat{S}_f^u points with larger U' learning function values (more likely to be misclassified) in the estimated failure domain are identified. Removing these \hat{S}_f^u points will cause the denominator N_f to decrease from \hat{N}_f to $\hat{N}_f - \hat{S}_f^u$. In addition, if the removed points contain the points with the largest likelihood function value, \hat{c}_2 should increase to c_2^* , causing more points in $\hat{\Omega}_f$ to "fail" according to LSFI. This increased \hat{c}_2 can be regarded as the upper bound of c_2^* and is denoted as c_2^u . It is calculated using the following equation:

$$c_2{}^u = \frac{1}{\max(L(x'^-))} \tag{30}$$

where x'^- represents the failure points in $\hat{\Omega}_f$ with the \hat{S}_f^u points removed. Let LSF2 denote the LSF1 with c_2 replaced by c_2^u . Note that the removed points may also contain the points that "fail" according to LSF2, resulting in a decrease in the numerator N_{f+} . To offset the impact, when considering the numerator, no point is actually removed, however, the numerator may still increase due to the adoption of c_2^u in LSF2. This is referred to as Case 2 where all the removed points did not fail according to LSF1. For the denominator, \hat{S}_f^u points are still removed. Therefore, $\frac{N_{f+}}{N_{e}}$ for the combined case (1 and 2) can be formulated as follows:

$$\left(\frac{N_{f+}}{N_f}\right)^{c12} = \frac{\widehat{N}_{f+u}}{\widehat{N}_f - \widehat{S}_f^u} \tag{31}$$

where \widehat{N}_{f+u} is the number of the points in the original $\widehat{\Omega}_f$ that "fail" according to LSF2. Nevertheless, this is not the true upper bound of $\frac{N_{f+}}{N_f}$, as if there are also points misclassified in $\hat{\Omega}_s$, the action of moving points from $\hat{\Omega}_s$ to $\hat{\Omega}_f$ can also potentially cause $\frac{N_{f+}}{N_f}$ to increase. This action will not only add the number of the added points from $\hat{\Omega}_s$ to $\hat{\Omega}_f$ to the denominator, but also add the number of the added points that fail according to LSF2 to the numerator. Let a denote \hat{N}_{f+u} and b denote $\hat{N}_f - \hat{S}_f^u$. It is obvious that b is often larger than a. Then let c denote the number of the added points from $\hat{\Omega}_s$ to $\hat{\Omega}_f$ that "fail" according to Eq. (28) with c_2^u and d denote the number of added points that do not "fail" according to Eq. (28) with c_2^u . Therefore, after adding c+d points to the failure domain, $\left(\frac{N_{f+}}{N_f}\right)^{c_{12}}$ can be written in the form of:

$$\frac{a+c}{b+c+d} = 1 - \frac{b-a+d}{b+c+d}$$
 (32)

This formula can be regarded as a function with respect to c and a function with respect to d, respectively. It is observed that the function with respect to c is monotonically increasing for $c \ge 0$ considering the right-hand side and the function with respect to d is monotonically decreasing for $d \ge 0$ considering the left-hand side. Hence after adding c + d points to the failure domain, $\left(\frac{N_{f+}}{N_f}\right)^{c_{12}}$ reaches its maximum when c reaches its maximum and d=0. This is denoted as Case 3 where all points among the \hat{S}^u_s points added from $\hat{\Omega}_s$ to $\hat{\Omega}_f$ are ones that "fail" according to LSF2. Note that the \hat{S}^u_s points are points with larger U' learning function values in $\hat{\Omega}_s$ and are identified similar to Case 1. In other words, $\frac{N_{f+}}{N_f}$ reaches its maximum when the combined case (1, 2 and 3), i.e., the extreme case, is considered. The upper bound of $\frac{N_{f+}}{N_f}$ will therefore have the following form:

$$\left(\frac{N_{f+}}{N_f}\right)^u = \frac{\widehat{N}_{f+u} + \widehat{N}_{f+ss}}{\widehat{N}_f - \widehat{S}_f^u + \widehat{N}_{f+ss}} \tag{33}$$

where \hat{N}_{f+ss} is the number of points in \hat{S}^u_s that fail according to LSF2

3.2 Lower bound of N_{f+}/N_f

The lower bound of $\frac{N_{f+}}{N_f}$ can be found in a similar fashion by first considering Case 4 where \hat{S}_s^u points in $\hat{\Omega}_s$ are misclassified. Adding \hat{S}_s^u points with larger U' learning function values to the failure domain will cause the denominator N_f to increase from \hat{N}_f . In addition, if the added points contain the points with the largest likelihood function value, \hat{c}_2 should decrease to c_2^* , causing fewer points in $\hat{\Omega}_f$ to fail according to *LSF1*. The decreased \hat{c}_2 can be regarded as the lower bound of c_2^* and is denoted as c_2^l . This term is determined using the following equation: $c_2^l = \frac{1}{max (L(x'^+))} \tag{34}$

$$c_2^l = \frac{1}{\max(L(x'^+))} \tag{34}$$

where x'^+ represents the failure points in $\hat{\Omega}_f$ with the \hat{S}_s^u points added. Let *LSF3* denote the *LSF1* where c_2 is replaced by c_2^l . Note that the added points may also contain the points that "fail" according to LSF3, causing an increase in the numerator N_{f+} . To offset the impact, when considering the numerator, no point is added, however, the numerator may still decrease due to the adoption of c_2^l in LSF3. This is referred to as Case 5 where all the added points did not fail according to LSF1. For the denominator, \hat{S}_s^u points are still added. Therefore, $\frac{N_{f+}}{N_f}$ for this extreme case can be formulated as follows:

$$\left(\frac{N_{f+}}{N_f}\right)^{ec45} = \frac{\widehat{N}_{f+l}}{\widehat{N}_f + \widehat{S}_s^u} \tag{35}$$

where \hat{N}_{f+l} is the number of the points in the original $\hat{\Omega}_f$ that fail according to LSF3. Similarly, this is not a true lower bound of $\frac{N_{f+}}{N_f}$, as the action of removing points from $\hat{\Omega}_f$ can potentially cause $\frac{N_{f+}}{N_f}$ to decrease. This action will subtract the number of the removed points from $\hat{\Omega}_f$ from the denominator and the number of the removed points that fail according to LSF3 from the numerator. Similarly, let e denote \hat{N}_{f+1} and f denote $\hat{N}_f + \hat{S}_s^u$. It is obvious that f is often larger than e. Then let g denote the number of the removed points from $\hat{\Omega}_f$ that "fail" according to LSF3 and h denote the number of the removed points that do not "fail" according to LSF3. So, after removing g + h points from the failure domain, $\left(\frac{N_{f+}}{N_f}\right)^{c45}$ can be written in the form of:

$$\frac{e - g}{f - g - h} = 1 - \frac{f - e - h}{f - g - h} \tag{36}$$

In the same fashion, this formula can be regarded as a monotonically decreasing function with respect to g for $g \ge 0$ considering the right-hand side and a monotonically increasing function with respect to h for $h \ge 0$ considering the left-hand side. Hence after moving g + h points to the failure domain, $\left(\frac{N_{f+}}{N_f}\right)^{c45}$ reaches its minimum when g reaches its maximum and h = 0. This is denoted as Case 6 where all points among the \hat{S}_s^u points added from $\hat{\Omega}_s$ to $\hat{\Omega}_f$ are the ones that "fail" according to LSF3. In other words, $\frac{N_{f+}}{N_f}$ reaches its minimum when the combined case (4, 5 and 6), i.e., the extreme case, is considered. The lower bound of $\frac{N_{f+}}{N_f}$ can therefore be determined as follows:

$$\left(\frac{N_{f+}}{N_f}\right)^l = \frac{\widehat{N}_{f+l} - \widehat{N}_{f+sf}}{\widehat{N}_f + \widehat{S}_s^u - \widehat{N}_{f+sf}}$$
(37)

where \hat{N}_{f+sf} is the number of points in \hat{S}_f^u that fail according to LSF3.

3.3 Posterior failure probability error

Since the upper and lower bounds of $\frac{N_{f+}}{N_f}$ are found, the estimation of the upper and lower bounds of $Pr(Z|E)^*/q$ is straightforward. The upper and lower bounds of c_2^* are also obtained during the process of estimating the range of $Pr(Z|E)^*/q$. The upper and lower bounds of $Pr(Z|E)^*/q$ can be easily calculated as the product of upper and lower bounds of $\frac{1}{c_2^*}$ and $\frac{N_{f+}}{N_f}$. Hence the maximum error of the Pr(Z|E) can be formulated using the following equation:

$$\hat{\epsilon}_{max}^{Pr(Z|E)} = max \left(\left| \frac{\frac{1}{\hat{c}_2} \frac{\widehat{N}_{f+}}{\widehat{N}_f} - \frac{1}{c_2^l} \left(\frac{N_{f+}}{N_f} \right)^u}{\frac{1}{c_2^l} \left(\frac{N_{f+}}{N_f} \right)^u} \right|, \left| \frac{\frac{1}{\hat{c}_2} \frac{\widehat{N}_{f+}}{\widehat{N}_f} - \frac{1}{c_2^u} \left(\frac{N_{f+}}{N_f} \right)^l}{\frac{1}{c_2^u} \left(\frac{N_{f+}}{N_f} \right)^l} \right| \right)$$
(38)

 \hat{P}'_f can be regarded as the product of \hat{P}_f and Pr(Z|E) divided by Pr(Z), where only the first two items introduce error. Once the estimate of the maximum error of $\hat{P}r(Z|E)$ is obtained, along with the maximum error of Pr(E), the maximum error of \hat{P}'_f can be determined as follows:

$$\hat{\epsilon}_{max}{}^{\hat{P}'_f} = \hat{\epsilon}_{max}{}^{P_f} + \hat{\epsilon}_{max}{}^{Pr(Z|E)} + \hat{\epsilon}_{max}{}^{P_f} \times \hat{\epsilon}_{max}{}^{Pr(Z|E)} \tag{39}$$

 $\hat{\epsilon}_{max}^{\ \ \ p'_f} = \hat{\epsilon}_{max}^{\ \ p'_f} + \hat{\epsilon}_{max}^{\ \ p_f} + \hat{\epsilon}_{max}^{\ \ p_f} \times \hat{\epsilon}_{max}^{\ \ \ p_f} \times \hat{\epsilon}_{max}^{\ \ \ p_f} \times \hat{\epsilon}_{max}^{\ \ \ \ p_f} \times \hat{\epsilon}_{max}^{\ \ \ \ \ \ \ \ \ \hat{\epsilon}_{max}^{\ \ \ \ \ \hat{\epsilon}_{max}^{\ \ \ \ \hat{\epsilon}_{max}^{\ \ \ \hat{\epsilon}_{max}^{\ \ \hat{\epsilon}_{max}^{\ \ \hat{\epsilon}_{max}^{\ \ \hat{\epsilon}_{max}^{\ \hat{\epsilon}_$ of failure, providing an accurate stopping criterion for training the surrogate model for estimation of the posterior probability of failure. A new reliability updating approach that adopts $\hat{\epsilon}_{max}^{\hat{p}'_f}$ as the stopping criterion is proposed, which will be introduced in the next section.

4. The Two-Phase RUAK approach

An approach for reliability updating with equality information with surrogate model is proposed in this section. In contrast to RUAK, the proposed method leverages the maximum error of posterior failure probability as the stopping criterion. In addition, a two-phase scheme is proposed here to improve the efficiency of the posterior failure probability estimation. According to Eq. (39), it can be observed that $\hat{\epsilon}_{max}^{Pr (E|Z)}$ is always larger than $\hat{\epsilon}_{max}^{Pr (Z|E)}$. Moreover, it requires more computations. Therefore, in the first phase, ESC is used to estimate the prior failure probability error until the error reaches the threshold of 5% like in the original RUAK. In the second phase, the posterior failure probability error is calculated to evaluate the proposed stopping criterion. The flowchart of the approach is shown in Fig. 1. The details of each step are summarized below:

- Step 1: Generating initial candidate design samples. First, N_{MCS} candidate design samples are generated using Latin Hypercube Sampling and the set of samples is denoted as S.
- Step 2: Initial training points. Randomly select an initial set of training points denoted as X_{tr} from S.
- Step 3: Phase 1 Kriging construction. Enter phase 1: Construct the Kriging meta-model $\hat{g}(X)$ with current X_{tr} . This construction is based on UQLab [30] in this paper.
- Step 4: Kriging prediction. The Kriging responses $\mu_{\hat{q}}(x)$ and variances $\sigma_{\hat{q}}^2(x_q)$ are obtained from the current Kriging model $\hat{g}(\mathbf{X})$ for every point in **S**. According to responses $\mu_{\hat{g}}(\mathbf{X})$, the failure probability \hat{P}_f is estimated via MCS.
- Step 5: Identification of the next training point. The point with the smallest value of U' learning function in S is selected as the next best training point.
- **Step 6**: Updating the training points. Add the identified next training point to X_{tr} .
- **Step 7**: Maximum error estimation of \hat{P}_f . Use ESC to estimate the maximum error of \hat{P}_f : $\hat{\epsilon}_{max}^{Pr(E)}$.

$$\hat{\epsilon}_{max}^{Pr(E)} \le \epsilon_{thr} \tag{40}$$

• Step 8: Checking the Phase 1 stopping criterion based on the maximum error. Check the stopping criterion: $\hat{\epsilon}_{max}^{Pr(E)} \leq \epsilon_{thr} \tag{40}$ where ϵ_{thr} is the error threshold. If the stopping criterion is not satisfied, then the process moves to Step 3; otherwise,

• Step 9: Checking the coefficient of variation of the failure probability. The sufficiency of the population of S is checked using:

$$COV_{\hat{P}_f} = \sqrt{\frac{1 - \hat{P}_f}{N_{MCS}\hat{P}_f}} \tag{41}$$

If $COV_{\hat{P}_f}$ is smaller than the predefined threshold 5%, then the process moves to Step 10. Otherwise, an additional number N_{Δ_S} of candidate design samples Δ_S should be added to S, and the process should move back to Step 4.

- Step 10: Phase 2 Kriging Construction. Enter Phase 2: Use the current X_{tr} to construct the Kriging meta-model
- Step 11: Kriging prediction. The Kriging responses $\mu_{\hat{q}}(x)$ and variances $\sigma_{\hat{q}}^2(x)$ are obtained from the current Kriging model $\hat{g}(X)$ for every point in **S**.
- Step 12: Identification of the next training point. The point with the smallest value of U' learning function is selected as the next best training point in S.
- **Step 13**: Updating the training points. Add the next training point to X_{tr} .
- **Step 14**: Maximum error estimation of \hat{P}'_f . Use Eq. (33), Eq. (37)-(39) to estimate the maximum error of \hat{P}'_f :
- Step 15: Checking the Phase 2 stopping criterion based on the maximum error. Check the stopping criterion: $\hat{\epsilon}_{max}^{Pr\ (E|Z)} \leq \epsilon_{thr}$ (4 If the stopping criterion is not satisfied, then the process moves to Step 10; otherwise, to Step 16.

$$\hat{\epsilon}_{max}^{Pr(E|Z)} \le \epsilon_{thr} \tag{42}$$

- Step 16: Calculating Pr(Z) and estimating P_f and Pr(Z|E). Pr(Z) can be calculated using Eq. (23) and P_f and Pr(Z|E) can be estimated using Eq. (21) and Eq. (26), respectively using the well-trained surrogate model $\hat{g}(X)$.
- Step 17: Estimating the posterior failure probability P'_f . Estimate the posterior failure probability using Eq. (20).

The proposed method avoids the unnecessary computation of $\hat{\epsilon}_{max}^{Pr(E|Z)}$ by adopting the two-phase scheme. The stopping criterion based on the maximum error of the posterior failure probability provides an accurate stop signal for the construction of surrogate model. The performance of the approach is demonstrated through four numerical examples in the next section.

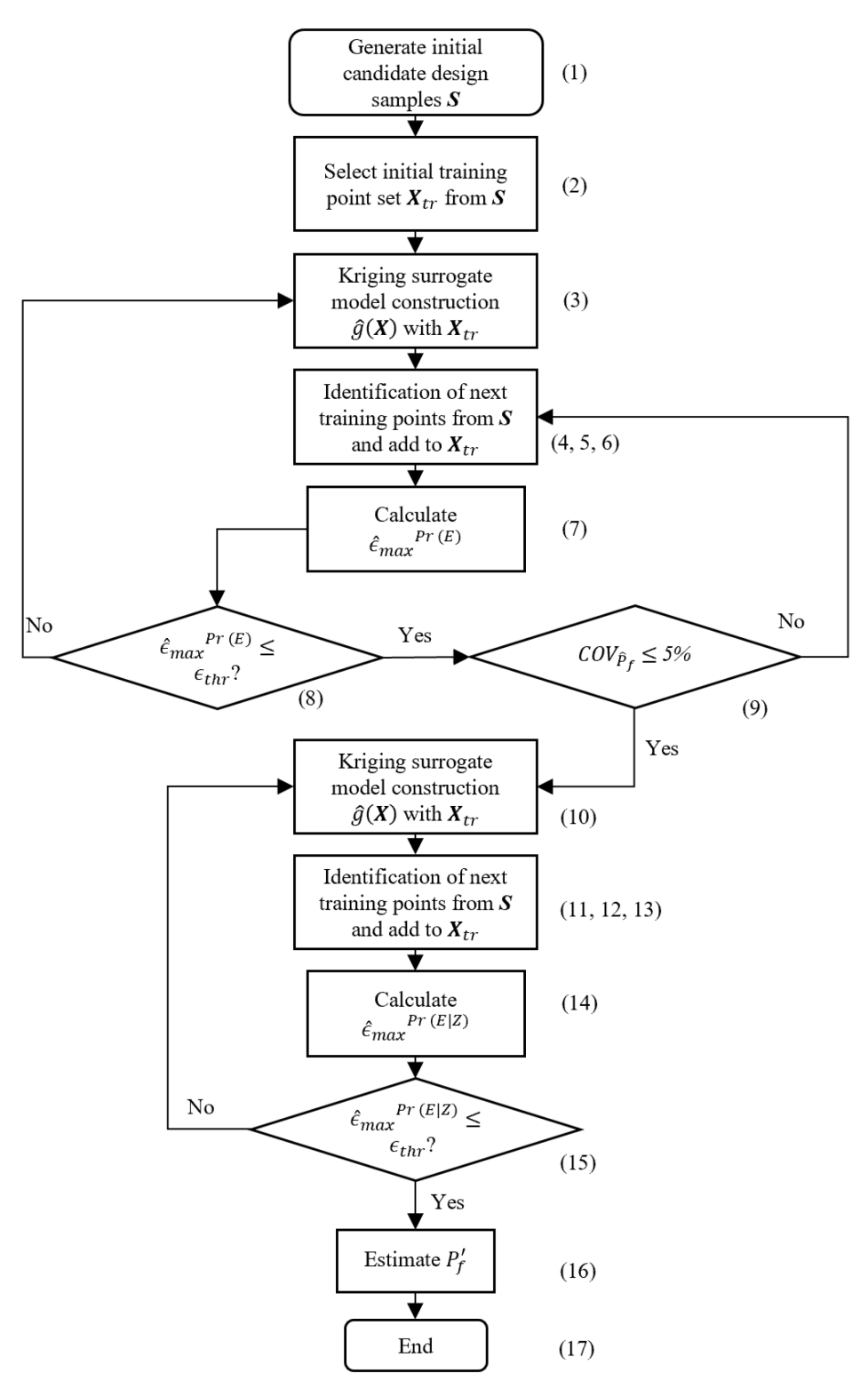


Fig.1 Flowchart of proposed approach

5. Numerical examples

In order to test the accuracy of the proposed approach, four numerical examples are investigated, and the results are compared with the original RUAK. The posterior failure probabilities obtained from crude MCS with 10⁶ function evaluations are used as the reference to calculate the error of the posterior failure probabilities obtained from RUAK and the proposed approach. For each example, the computation is repeated 30 times. To offset the impact of the randomness introduced by the auxiliary standard uniform random variable p, the three methods share the same realization of p in each computation.

5.1. Linear and normal case

The first example investigates the performance of reliability updating methods for a linear problem involving multiple normal random variables [19]. The limit state function is defined as:

$$g(\mathbf{X}) = 2X_1 + 3X_2 + 6X_3 + 4X_4 - X_5 - 2X_6 - 4X_7 - 4X_8 \tag{43}$$

 $g(X) = 2X_1 + 3X_2 + 6X_3 + 4X_4 - X_5 - 2X_6 - 4X_7 - 4X_8$ where $X = [X_1, ..., X_8]$ are identically distributed independent normal random variables with mean $\mu_X = 10$ and standard deviation $\sigma_X = 2$. In this example, three observations are considered with measurement errors ε_{m1} , ε_{m2} , and ε_{m3} , respectively. The equality information is described by the following functions:

$$h_i(x_i, x_{i+1}, \varepsilon_{mi}) = x_i + x_{i+1} - 20 + \varepsilon_{mi}, i = 1, 2, 3$$
 (44)

All three measurement errors are identical independent standard normal random variables. Thus, the likelihood function can be formulated as follows:

$$L(\mathbf{x}) = \prod_{i=1}^{3} L_i(x_i, x_{i+1}) = \prod_{i=1}^{3} \varphi(20 - x_i - x_{i+1})$$
 (45)

where φ is the probability density function of the standard normal variable, x_1, x_2, x_3 and x_4 are samples of X_1, X_2, X_3 and X_4 , respectively. For all problems in this section, the threshold of the stopping criterion is set as $\epsilon_{thr} = 0.05$, the coefficient of variation of \hat{P}_f is also set as 0.05, the number of initial training samples randomly chosen using LHS is 12, and the initial number of candidate design points is $N_S = 10^4$ with $N_{\Delta_S} = 10^4$.

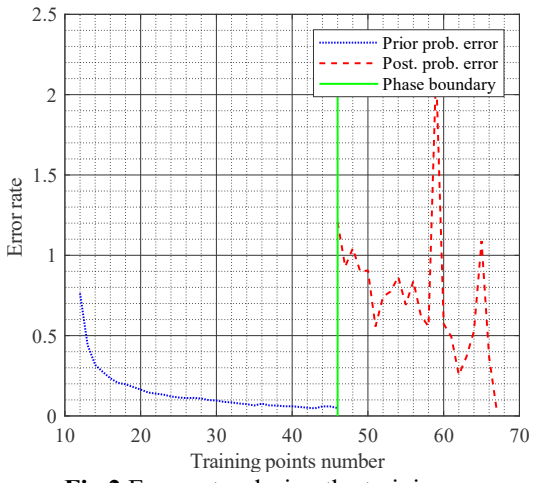


Fig.2 Error rates during the training process for the Two-Phase approach

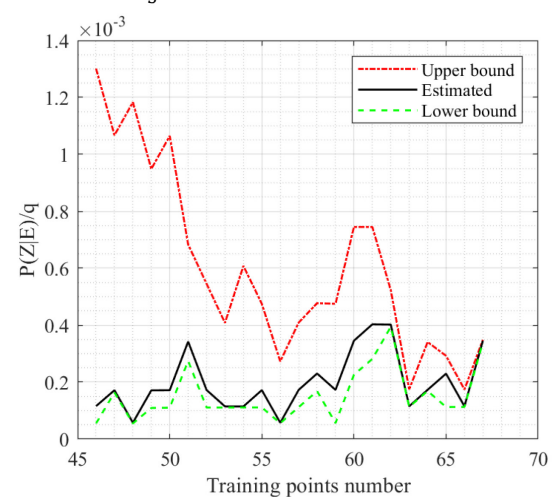


Fig.3 Upper and lower bounds for $Pr(Z|E)^*/q$ during the training process

The results for the proposed method are summarized in Table 1 and are compared with the results obtained using RUAK. Both approaches use UQLab [30] for the surrogate model construction and share the same configuration. This process is also applied to the other examples. Results are based on repeating the computations 30 times. The error is based on the comparison between the posterior failure probability determined using the considered approaches and MCS. Fig. 2 shows the error rates during the training process for the proposed approach. As shown in the figure, in the first phase, the maximum error rate for the prior failure probability is recorded until it reaches the 5% threshold. In the second phase, the training process continues until the maximum error rate for the posterior probability error is less than the 5% threshold. Fig. 3 shows the upper and lower bounds for $Pr(Z|E)^*/q$ during the training process of the second phase. The curve in the middle is the estimated value, which lies between the upper and lower bounds. It can be observed that in both Fig. 2 and Fig. 3 there are fluctuations in the curves for the second phase. This fluctuation is expected due to the randomness introduced by the auxiliary standard uniform random variable p. A "bad" realization of a set of p may lead to a quite slow convergence rate. Thus, in each iteration of the approach, a different set of p is generated to avoid potential slow convergence, hence the fluctuations. It is seen that the proposed approach substantially reduces both the average and maximum error compared to RUAK. As shown in the Table 1, the average error rate of the 30 runs with the original RUAK is 6.5%, which exceeds the predefined threshold, while the one with the Two-Phase RUAK is 2.1%, which is controlled under the threshold. Using the original RUAK, the maximum error from 30 replicate sets is 23.3%, while this error using the Two-Phase RUAK is limited to 5.6%.

Table 1 Reliability updating results for the linear and normal example based on 30 replicate sets

Methodology	Posterior failure probability average	Number of function calls	Average error	Maximum error
MCS	1.1×10^{-3}	10^{6}	-	-
RUAK	1.1×10^{-3}	40-49	6.5%	23.3%
Two-Phase RUAK	1.1×10^{-3}	54-75	2.1%	5.6%

5.2. Structural system case

The second example is a classical structural system problem studied by many researchers [32], [33]. The problem investigates an elastoplastic frame that is subject to a horizontal load H and a vertical load V as shown in Fig. 4. It is a series system reliability problem considering three failure mechanisms: sway, beam, and combined mechanisms. The plastic-moment capacities of this structure are denoted by R_1, R_2, \dots, R_5 . The limit state functions corresponding to the three mechanisms can be easily obtained through plastic analysis. The limit state function of the system can be defined as the minimum of three limit state functions as follows:

$$g(V, H, \mathbf{R}) = min \begin{cases} R_1 + R_2 + R_4 + R_5 - 5H \\ R_2 + 2R_3 + R_4 - 5V \\ R_1 + 2R_3 + 2R_4 + R_5 - 5H - 5V \end{cases}$$
 where H follows the Gumbel distribution, V follows the Gamma distribution and $R_1, R_2, ..., R_5$ all follow the

lognormal distribution and are correlated. The properties of the random variables are summarized in Table 2.

Table 2 Random variables in structural system example

Random variable	Distribution type	Mean	C.O.V	Correlation
$R_i, i = 1, \dots, 5(kN.m)$	Joint Lognormal	150	0.2	$ \rho_{\ln R} = 0.3 $
H(kN)	Gumbel	50	0.4	Independent
<i>V</i> (kN)	Gamma	60	0.2	Independent

Two measurements M_4 and M_5 are considered for R_4 and R_5 , respectively. The corresponding measurement errors ε_{m4} and ε_{m5} both follow independent normal distributions with a mean of 0 and a standard deviation of 15 kN.m. The equality information can be described by the following equations:

$$h_i(R_i, \varepsilon_{mi}) = R_i - M_i + \varepsilon_{mi}, i = 4,5 \tag{47}$$

where M_4 and M_5 are taken as 150 kN. m and 200 kN. m, respectively. Thus, the corresponding likelihood function can be formulated as:

$$L(\mathbf{r}) = \varphi^*(M_4 - r_4) \cdot \varphi^*(M_5 - r_5)$$
(48)

where r_4 and r_5 are samples from R_4 and R_5 , and φ^* is the probability density function of normal distribution with mean 0 and standard deviation of 15 kN. m. In the implementation of both approaches, the number of initial training samples is set to 12 and the initial number of candidate design points is $N_S = 10^4$ with $N_{\Delta S} = 10^4$. The results of this case based on 30 replicate sets are presented in Table 3.

As shown in Table 3, the average error of Two-Phase RUAK is 2.5%, which is below the threshold of 5%. On the other hand, the original RUAK has an average error of 8.3%. Moreover, the maximum error of the original RUAK reaches 46.6% while the Two-Phase RUAK has a maximum error of 12.4%. For the original RUAK, the average of the posterior failure probabilities from 30 computations is different from the one derived using MCS, while the average of the posterior failure probabilities from two-phase RUAK is the same as MCS.

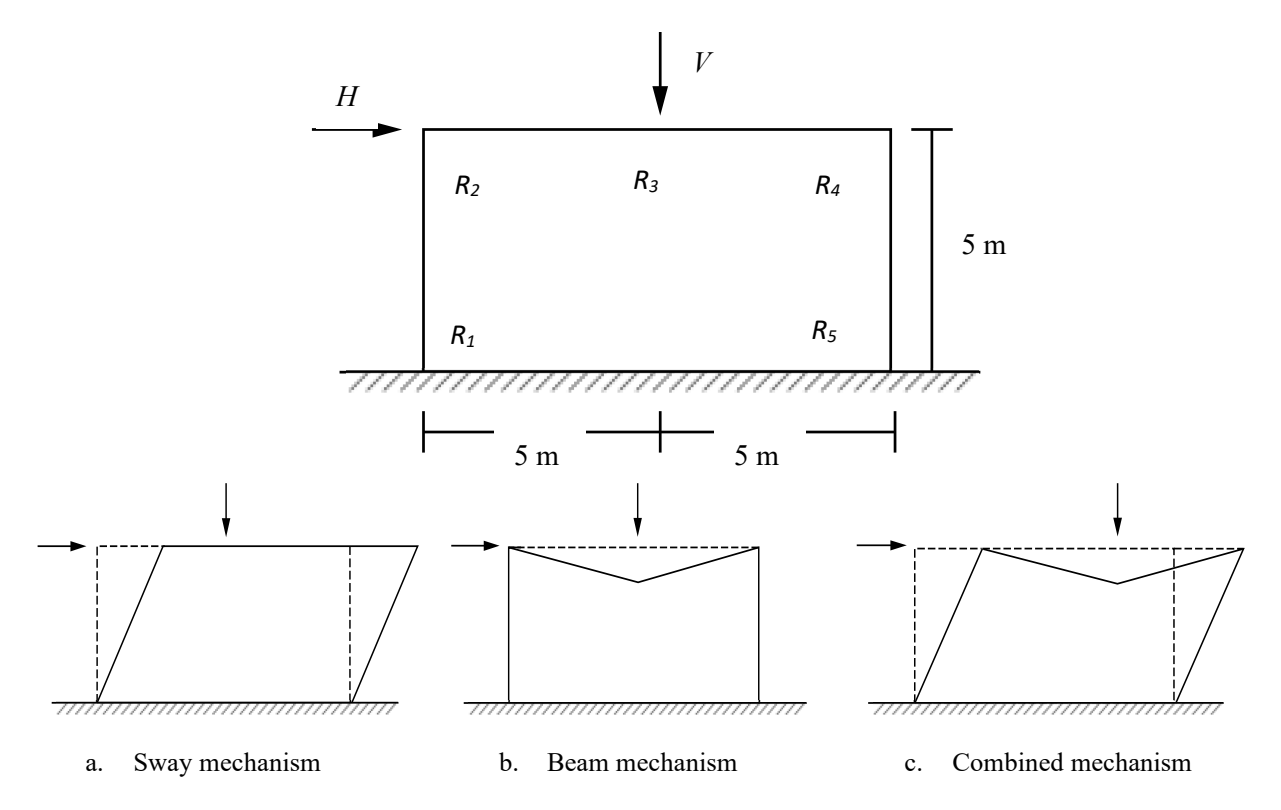


Fig. 4 Ductile structural frame with three failure mechanisms

Table 3 Reliability updating results for the structural system example based on 30 replicate sets.

Methodology	Posterior failure probability average	Number of function calls	Average error	Maximum error
MCS	6.9×10^{-3}	10^{6}	-	-
RUAK	6.7×10^{-3}	43-117	8.3%	46.6%
Two-Phase RUAK	6.9×10^{-3}	92-261	2.5%	6.4%

5.3. Example with 10 dimensions and multiple measurements

The third example is a 23-bar truss bridge with ten input random variables [34], [35]. The example investigates reliability updating with multiple measurements. As shown in Fig. 5, the bridge, which consists of 11 horizontal bars and 12 diagonal bars, is subject to 6 vertical forces $P = [P_1, ..., P_6]$. A_1 and A_2 are the cross-sectional areas of horizontal and diagonal bars, respectively, and E_1 and E_2 are the corresponding Young's moduli. All the random variables are stored in a vector $X = [P_1, P_2, P_3, P_4, P_5, P_6, A_1, A_2, E_1, E_2]$. The limit state function of the problem is as follows:

$$g(\mathbf{X}) = 0.14 - |dis(\mathbf{X})| \tag{49}$$

where dis(X) is the displacement at the midpoint and is calculated using matrix structural analysis. The probabilistic information of the ten independent random variables in X can be found in Table 4. For this example, the number of initial training samples is set to 12 and the initial number of candidate design points is $N_S = 10^4$ with $N_{\Delta S} = 10^4$. Four measurements of P_1 , P_2 , A_1 and A_2 are considered with the corresponding errors ε_{m1} and ε_{m2} , which both follow a normal distribution with mean 0 and standard deviation 0.5×10^4 N and ε_{m3} and ε_{m4} , which follow a normal distribution with mean 0 and standard deviation 1×10^{-4} m². The information functions can be expressed as follows:

$$h_{1}(P_{1}, \varepsilon_{m1}) = P_{1} - 8.5 \times 10^{4} + \varepsilon_{m1}$$

$$h_{2}(P_{2}, \varepsilon_{m1}) = P_{2} - 7.5 \times 10^{4} + \varepsilon_{m2}$$

$$h_{3}(A_{1}, \varepsilon_{m3}) = A_{1} - 1.85 \times 10^{-3} + \varepsilon_{m3}$$

$$h_{4}(A_{2}, \varepsilon_{m4}) = A_{2} - 0.9 \times 10^{-3} + \varepsilon_{m4}$$
(50)

Therefore, the corresponding likelihood function can be represented as:

$$L(x) = \varphi^{1,2}(\varepsilon_{m1}) \cdot \varphi^{1,2}(\varepsilon_{m2}) \cdot \varphi^{3,4}(\varepsilon_{m3}) \cdot \varphi^{3,4}(\varepsilon_{m4})$$

$$= \varphi^{1,2}(8.5 \times 10^4 - P_1) \cdot \varphi^{1,2}(7.5 \times 10^4 - P_6) \cdot \varphi^{3,4}(1.85 \times 10^{-3} - A_1) \cdot \varphi^{3,4}(0.9 \times 10^{-3} - A_2)$$
(51)

where $\varphi^{1,2}$ is the probability density function of normal distribution with mean 0 and standard deviation 0.5×10^4 and $\varphi^{3,4}$ is the probability density function of normal distribution with mean 0 and standard deviation 1×10^{-4} .

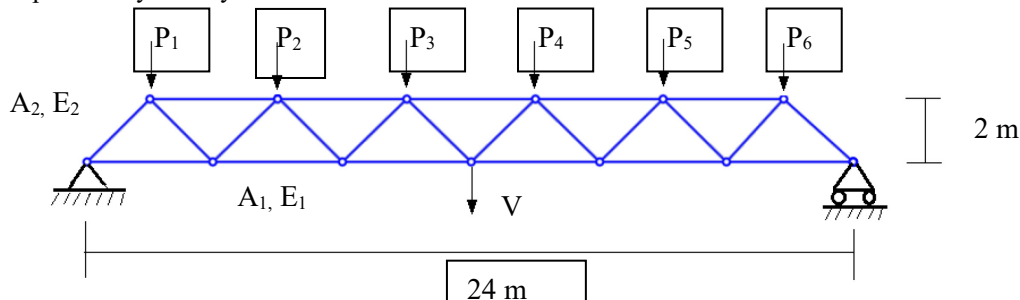


Fig. 5 Truss bridge with the example

Table 4. Random variables in ten-dimensional example with multiple measurements.

Random variable	Distribution	Mean	Standard deviation
$P_1 - P_6 (N)$	Gumbel	6.5×10^4	6.5×10^{3}
A_1 (m ²)	Lognormal	2×10^{-3}	2×10^{-4}
A_2 (m ²)	Lognormal	1×10^{-3}	1×10^{-4}
E_1 (Pa)	Lognormal	2.1×10^{11}	2.1×10^{10}
E_2 (Pa)	Lognormal	2.1×10^{11}	2.1×10^{10}

The results for this example are summarized in Table 5. It is evident that with slightly more training points, the average error of Two-Phase RUAK is 43% smaller than that of RUAK. Moreover, Two-Phase RUAK has the maximum error of 5.6%, while the maximum error of RUAK is 11.9%.

Table 5. Reliability updating results for 10-dimensional example based on 30 replicate sets.

Methodology	Posterior failure probability average	Number of function calls	Average error	Maximum error
MCS	1.25×10^{-2}	10^{6}	-	-
RUAK	1.26×10^{-2}	74-97	3.7%	11.9%
Two-Phase RUAK	1.25×10^{-2}	87-122	2.1%	5.6%

5.4. Oscillator example

The last example is an un-damped single degree of freedom system with six random variables as shown in Fig. 6. The details of this model can be found in [11], [36]–[39]. The performance function is described below:

$$g(k_1, k_2, m, r, t_1, F_1) = 3r - \left| \frac{2F_1}{m\omega_0^2} \sin\left(\frac{\omega_0 t_1}{2}\right) \right|$$
 (52)

where ω_0 is the system frequency and is calculated using $\sqrt{\frac{k_1+k_2}{m}}$. All random variables in this example follow normal

distributions. The properties of the six random variables are summarized in Table 6. In this example, two observations are considered with measurement errors of ε_{m_1} and ε_{m_2} . The equality information is described by the following function:

$$h_1(r) = r - 1 + \varepsilon_{m_1} h_2(F_1) = F_1 - 0.9 + \varepsilon_{m_2}$$
(53)

The measurement errors are statistically independent and identical normal random variables with the mean of 0 and the standard deviation of 10^{-1} . Thus, the likelihood function can be formulated as follows:

$$L(\mathbf{x}) = \varphi^*(1 - x_r) \cdot \varphi^*(1 - x_{F_1})$$
(54)

where φ^* is the probability density function of the normal distribution with mean of 0 and standard deviation of 10^{-1} , x_r and x_{F_1} are samples of r and F_1 , respectively. For this example, the number of initial training samples is set to 12 and the initial number of candidate design points is $N_S = 10^6$.

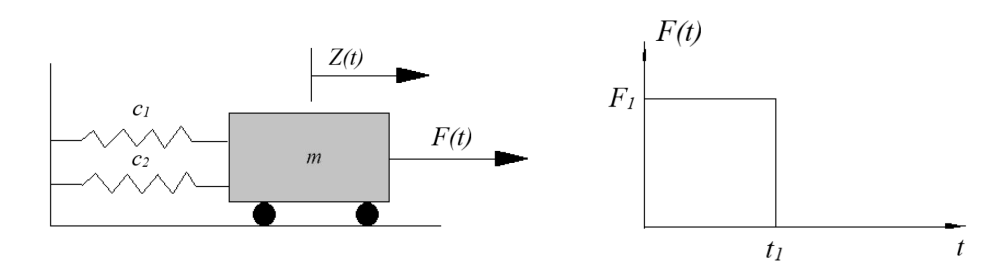


Fig. 6 Oscillator

Table 6. Random variables in nonlinear oscillator.

Random variable	Distribution	Mean	Standard deviation
\overline{m}	Normal	1	0.05
k_1	Normal	1	0.1
k_2	Normal	0.1	0.01
r	Normal	0.5	0.05
F_1	Normal	1	0.2
t_1	Normal	1	0.2

The results for this example are summarized in Table 7. It is demonstrated that the original RUAK, when dealing with this problem with extremely low posterior probability of failure, cannot effectively control the errors of the final output. The average error of RUAK has reached 22.4% and the maximum error is as high as 47.7%. The proposed method, on the other hand, effectively controls the errors using the developed more accurate stopping criterion for the posterior failure probability. The average of the posterior failure probabilities based on 30 replicate sets by the proposed the method is exactly the same as the reference by MCS, while the one by RUAK is smaller.

Table 7. Reliability updating results for nonlinear oscillator based on 30 replicate sets.

Methodology	Posterior failure probability average	Number of function calls	Average error	Maximum error
MCS	2.8×10^{-5}	10^{7}	-	-
RUAK	3.2×10^{-5}	24-28	22.4%	47.7%
Two-Phase RUAK	2.8×10^{-5}	77-149	0.4%	0.9%

6. Conclusions

This paper introduces a method to calculate the posterior failure probability error, and a two-phase RUAK approach that takes advantage of the posterior failure probability error estimation. The error estimation of the final output allows a stopping criterion for the Kriging model construction that assures desired accuracy for reliability updating. The two-phase scheme minimizes the computational demand in achieving the desired accuracy. Four numerical examples, including a linear and normal problem, a structural system and a ten-dimensional problem with multiple measurements are investigated to examine the accuracy improvement of the proposed approach. For each example, the calculation is repeated 30 times to test the robustness. It is observed that the average errors of the final outputs of the proposed method are significantly smaller and the maximum errors are contained more effectively compared to the state-of-the-art method RUAK. The fact that the error-based stopping criterion used in RUAK is not able to capture the actual posterior failure probability error sometimes leads to premature stops of the refinement of the surrogate model, meanwhile the proposed method vields significantly more accurate results at the cost of more computational costs.

Appendix

As noted in Eq. (20) \hat{P}'_f is the product of \hat{P}_f and Pr(Z|E) divided by Pr(Z). It should be noted that Pr(Z) does not involve the Kriging model. Therefore, the error introduced in \hat{P}'_f as a result of the Kriging model, only \hat{P}_f and Pr(Z|E)

are of interest. It is obvious the following equation holds:
$$\hat{P}'_f = \frac{\widehat{Pr}(Z|E)\widehat{P}_f}{Pr(Z)} = \frac{Pr(Z|E)P_f \times \left(1 \pm \hat{\epsilon}^{P(Z|E)}\right) \times (1 \pm \hat{\epsilon}^{P_f})}{Pr(Z)}$$
(55)

where $\hat{\epsilon}^{P(Z|E)}$ and $\hat{\epsilon}^{Pf}$ are the error of Pr(Z|E) and \hat{P}_f caused by the Kriging model, respectively. The actual posterior failure probability P'_f can be expressed using the following equation:

$$P_f' = \frac{Pr(Z|E)P_f}{Pr(Z)} \tag{56}$$

Dividing Eq. (55) by Eq. (56), we have:

$$1 + \hat{\epsilon}^{\hat{P}_f'} = \frac{\hat{P}_f'}{P_f'} = \left(1 \pm \hat{\epsilon}^{P(Z|E)}\right) \times \left(1 \pm \hat{\epsilon}^{P_f}\right) \tag{57}$$

As both
$$\hat{\epsilon}^{P(Z|E)}$$
 and $\hat{\epsilon}^{Pf}$ are positive by definition, the following equation holds:

$$(1 \pm \hat{\epsilon}^{P(Z|E)}) \times (1 \pm \hat{\epsilon}^{Pf}) \leq (1 + \hat{\epsilon}^{P(Z|E)}) \times (1 + \hat{\epsilon}^{Pf}) = 1 + \hat{\epsilon}^{P(Z|E)} + \hat{\epsilon}^{Pf} + \hat{\epsilon}^{P(Z|E)} \times \hat{\epsilon}^{Pf}$$
(58)

Combining Eq. (57) an Eq. (58), we have:

$$\hat{\epsilon}^{\hat{P}_f'} \le \hat{\epsilon}^{P(Z|E)} + \hat{\epsilon}^{P_f} + \hat{\epsilon}^{P(Z|E)} \times \hat{\epsilon}^{P_f} \tag{59}$$

Taking the maxima of all elements in Eq. (54), we have Eq. (39).

Acknowledgments

This research has been partly funded by the U.S. National Science Foundation (NSF) through awards CMMI-1635569, 1762918, and 2000156. In addition, this work is supported in part by Lichtenstein endowment at The Ohio State University. These supports are greatly appreciated.

Reference

- S. Marelli, R. Schöbi, and B. Sudret, "UQLab User Manual Structural Reliability (Rare Events Estimation)," [1]
- [2] O. Ditlevsen and H. O. Madsen, Structural reliability methods, vol. 178. Wiley New York, 1996.
- M. Lemaire, Structural reliability. John Wiley & Sons, 2013. [3]
- R. Y. Rubinstein and D. P. Kroese, Simulation and the Monte Carlo method. John Wiley & Sons, 2016. [4]
- [5] V. J. Romero, L. P. Swiler, and A. A. Giunta, "Construction of response surfaces based on progressive-latticesampling experimental designs with application to uncertainty propagation," Struct. Saf., vol. 26, no. 2, pp. 201–219, 2004.
- A. A. Giunta, J. M. McFarland, L. P. Swiler, and M. S. Eldred, "The promise and peril of uncertainty [6] quantification using response surface approximations," Struct. Infrastruct. Eng., vol. 2, no. 3–4, pp. 175–189,
- W. Zhao, F. Fan, and W. Wang, "Non-linear partial least squares response surface method for structural reliability analysis," Reliab. Eng. Syst. Saf., vol. 161, pp. 69-77, May 2017, doi: 10.1016/j.ress.2017.01.004.
- G. Blatman and B. Sudret, "An adaptive algorithm to build up sparse polynomial chaos expansions for stochastic finite element analysis," Probabilistic Eng. Mech., vol. 25, no. 2, pp. 183-197, 2010.
- J.-M. Bourinet, "Rare-event probability estimation with adaptive support vector regression surrogates," Reliab. Eng. Syst. Saf., vol. 150, pp. 210–221, 2016.
- [10] H. Dai, H. Zhang, W. Wang, and G. Xue, "Structural reliability assessment by local approximation of limit state functions using adaptive Markov chain simulation and support vector regression," Comput.-Aided Civ. Infrastruct. Eng., vol. 27, no. 9, pp. 676–686, 2012.
- [11] B. Echard, N. Gayton, and M. Lemaire, "AK-MCS: an active learning reliability method combining Kriging and Monte Carlo simulation," Struct. Saf., vol. 33, no. 2, pp. 145–154, 2011.
- [12] D. R. Jones, M. Schonlau, and W. J. Welch, "Efficient Global Optimization of Expensive Black-Box Functions," J. Glob. Optim., vol. 13, no. 4, pp. 455-492, Dec. 1998, doi: 10.1023/A:1008306431147.
- [13] B. J. Bichon, M. S. Eldred, L. P. Swiler, S. Mahadevan, and J. M. McFarland, "Efficient global reliability analysis for nonlinear implicit performance functions," AIAA J., vol. 46, no. 10, pp. 2459–2468, 2008.
- [14] J. Bect, D. Ginsbourger, L. Li, V. Picheny, and E. Vazquez, "Sequential design of computer experiments for the estimation of a probability of failure," Stat. Comput., vol. 22, no. 3, pp. 773–793, May 2012, doi: 10.1007/s11222-011-9241-4.

- [15] V. Picheny, D. Ginsbourger, O. Roustant, R. T. Haftka, and N.-H. Kim, "Adaptive Designs of Experiments for Accurate Approximation of a Target Region," *J. Mech. Des.*, vol. 132, no. 7, p. 071008, Jul. 2010, doi: 10.1115/1.4001873.
- [16] B. Gaspar, A. P. Teixeira, and C. G. Soares, "Assessment of the efficiency of Kriging surrogate models for structural reliability analysis," *Probabilistic Eng. Mech.*, vol. 37, pp. 24–34, Jul. 2014, doi: 10.1016/j.probengmech.2014.03.011.
- [17] B. Gaspar, A. P. Teixeira, and C. Guedes Soares, "Adaptive surrogate model with active refinement combining Kriging and a trust region method," *Reliab. Eng. Syst. Saf.*, vol. 165, pp. 277–291, Sep. 2017, doi: 10.1016/j.ress.2017.03.035.
- [18] M. Xiao, J. Zhang, and L. Gao, "A system active learning Kriging method for system reliability-based design optimization with a multiple response model," *Reliab. Eng. Syst. Saf.*, vol. 199, p. 106935, Jul. 2020, doi: 10.1016/j.ress.2020.106935.
- [19] D. Straub, "Reliability updating with equality information," *Probabilistic Eng. Mech.*, vol. 26, no. 2, pp. 254–258, Apr. 2011, doi: 10.1016/j.probengmech.2010.08.003.
- [20] Z. Wang and A. Shafieezadeh, "Real-time high-fidelity reliability updating with equality information using adaptive Kriging," *Reliab. Eng. Syst. Saf.*, vol. 195, p. 106735, Mar. 2020, doi: 10.1016/j.ress.2019.106735.
- [21] H. O. Madsen, "Model updating in reliability theory," presented at the ICASP 5, 1987.
- [22] S. Gollwitzer, B. Kirchgäßner, R. Fischer, and R. Rackwitz, "PERMAS-RA/STRUREL system of programs for probabilistic reliability analysis," *Struct. Saf.*, vol. 28, no. 1, pp. 108–129, Jan. 2006, doi: 10.1016/j.strusafe.2005.03.008.
- [23] Z. Wang and A. Shafieezadeh, "ESC: an efficient error-based stopping criterion for kriging-based reliability analysis methods," *Struct. Multidiscip. Optim.*, Nov. 2018, doi: 10.1007/s00158-018-2150-9.
- [24] Z. Wang and A. Shafieezadeh, "REAK: Reliability analysis through Error rate-based Adaptive Kriging," *Reliab. Eng. Syst. Saf.*, vol. 182, pp. 33–45, Feb. 2019, doi: 10.1016/j.ress.2018.10.004.
- [25] C. Zhang, Z. Wang, and A. Shafieezadeh, "Value of Information Analysis via Active Learning and Knowledge Sharing in Error-Controlled Adaptive Kriging," *IEEE Access*, vol. 8, pp. 51021–51034, 2020, doi: 10.1109/ACCESS.2020.2980228.
- [26] G. Li, H. Yang, and G. Zhao, "A new efficient decoupled reliability-based design optimization method with quantiles," *Struct. Multidiscip. Optim.*, vol. 61, no. 2, pp. 635–647, Feb. 2020, doi: 10.1007/s00158-019-02384-7.
- [27] M. Moustapha, B. Sudret, J.-M. Bourinet, and B. Guillaume, "Quantile-based optimization under uncertainties using adaptive Kriging surrogate models," *Struct. Multidiscip. Optim.*, vol. 54, no. 6, pp. 1403–1421, Dec. 2016, doi: 10.1007/s00158-016-1504-4.
- [28] T. J. Santner, B. J. Williams, and W. I. Notz, *The Design and Analysis of Computer Experiments*. New York: Springer-Verlag, 2003.
- [29] S. N. Lophaven, H. B. Nielsen, and J. Søndergaard, "DACE A Matlab Kriging Toolbox, Version 2.0," Report, 2002.
- [30] "UQLab Kriging (Gaussian process modelling) manual," *UQLab, the Framework for Uncertainty Quantification*. http://www.uqlab.com/userguidekriging (accessed May 13, 2017).
- [31] M. Gen and L. Lin, "Genetic Algorithms," in *Wiley Encyclopedia of Computer Science and Engineering*, American Cancer Society, 2008, pp. 1–15.
- [32] Straub Daniel and Der Kiureghian Armen, "Bayesian Network Enhanced with Structural Reliability Methods: Application," *J. Eng. Mech.*, vol. 136, no. 10, pp. 1259–1270, Oct. 2010, doi: 10.1061/(ASCE)EM.1943-7889.0000170.
- [33] "Engineering Design Reliability Handbook," *CRC Press*, Dec. 22, 2004. https://www.crcpress.com/Engineering-Design-Reliability-Handbook/Nikolaidis-Ghiocel-Singhal/p/book/9780849311802 (accessed May 19, 2018).
- [34] J. Wang, Z. Sun, Q. Yang, and R. Li, "Two accuracy measures of the Kriging model for structural reliability analysis," *Reliab. Eng. Syst. Saf.*, vol. 167, pp. 494–505, Nov. 2017, doi: 10.1016/j.ress.2017.06.028.
- [35] N. Roussouly, F. Petitjean, and M. Salaun, "A new adaptive response surface method for reliability analysis," *Probabilistic Eng. Mech.*, vol. 32, pp. 103–115, Apr. 2013, doi: 10.1016/j.probengmech.2012.10.001.
- [36] S. K. Au and J. L. Beck, "Subset simulation and its application to seismic risk based on dynamic analysis," *J. Eng. Mech.*, vol. 129, no. 8, pp. 901–917, 2003.
- [37] L. Schueremans and D. Gemert, "Benefit of splines and neural networks in simulation based structural reliability analysis," 2005, doi: 10.1016/j.strusafe.2004.11.001.

- [38] M. R. Rajashekhar and B. R. Ellingwood, "A new look at the response surface approach for reliability analysis," *Struct. Saf.*, vol. 12, no. 3, pp. 205–220, 1993.
- [39] N. Gayton, J. M. Bourinet, and M. Lemaire, "CQ2RS: a new statistical approach to the response surface method for reliability analysis," *Struct. Saf.*, vol. 25, no. 1, pp. 99–121, Jan. 2003, doi: 10.1016/S0167-4730(02)00045-0.